Geochimica et Cosmochimica Acta Vol. 55, pp. 441–456

0016-7037/91/$3.00 + .00

Diffusion of water in rhyolitic glasses

YOUXUE ZHANG, E. M. STOLPER, and G. J. WASSERBURG
Division of Geological and Planetary Sciences, California Institute of Technology, Pasadena, CA 91125, USA

(*Received March* 19, 1990; *accepted in revised form November* 5, 1990)

Abstract—Water dehydration experiments on rhyolitic glasses have been carried out at 400–550°C under a N_2 atmosphere. Concentration profiles of both H_2O molecules and OH groups were measured by Fourier transform infrared spectroscopy. As found in previous studies of water diffusion in rhyolitic melts, the measured total water concentration profiles do not match expectations based on a single constant diffusion coefficient for total water.

The diffusion of total water is described by considering the diffusion of both H_2O molecules and OH groups and the reaction between them. The concentration relationship between the two species has been obtained from direct infrared measurement on quenched experimental charges. The quench is inferred to be rapid enough to preserve concentrations of both species at experimental temperature based on experimental results designed to examine reaction kinetics. The measured species concentrations along diffusion profiles show that local equilibrium between H_2O and OH is approximately reached at high temperatures and high water contents. However, at lower water content or lower temperature, local equilibrium is not reached. In treating the diffusion problem, this disequilibrium effect is partially compensated by using empirical relationships between H_2O and OH concentrations based on measurements, instead of using an equilibrium relationship. It is thus possible to obtain diffusion coefficients for both species from their concentration profiles. The diffusion coefficient of OH is found to be negligible compared to that of H_2O at 403–530°C ($D_{OH} < 0.02 D_{H_2O}$ and could be much smaller); i.e., H_2O is the dominant diffusing species even at total water concentration as low as 0.2 wt%. The variation of OH concentration along the diffusion profile is inferred to be due to the local interconversion between OH groups and H_2O molecules; the reaction also provides the diffusing H_2O species. D_{H_2O} values are found to vary by less than a factor of 2 over a total water concentration range of 0.2 to 1.7 wt%. This simple model, coupled with the assumption of local equilibrium between H_2O and OH, yields a very good fit to the data from diffusion-couple experiments of LAPHAM et al. (1984) at 850°C. When our data are combined with D_{H_2O} obtained from that fit, D_{H_2O} (in m^2/s) is given by

$$\ln D_{H_2O} = (-14.59 \pm 1.59) - (103000 \pm 5000)/RT$$

$$673\ \text{K} \le T \le 1123\ \text{K}$$

where T is temperature in K and R is the gas constant in J K^{-1} mol^{-1}. This equation also approximates well D_{H_2O} values calculated from previous measurements of concentration-dependent bulk water diffusion coefficients of KARSTEN et al. (1982). The diffusion of H_2O is also compared to the diffusion of the noble gas elements. The activation energy for diffusion in rhyolitic glasses is well correlated with neutral species radii of He, Ne, H_2O, and Ar. This supports the contention that the diffusing species for "water" is neutral molecular H_2O. The role of speciation may also be important in understanding the diffusion of many other multi-species components, and the effect can be treated in a similar fashion as that during water diffusion.

INTRODUCTION

DIFFUSIVE TRANSPORT OF WATER in silicate liquids and glasses plays an important role in a number of phenomena of interest in the geological and materials sciences. For example, the rate of water diffusion in silicate liquids is a critical factor in the growth of bubbles in ascending magmas, and thus may influence the degree to which magmas can dehydrate on ascent and the availability of compressed vapor in bubbles to power explosive volcanic eruptions. Hydration and dehydration of silicate glasses in geological and man-made environments are also limited by water diffusion, and relate to several important issues including the chemical stability of glasses, the mechanical strength of glass fibers, water-rock reaction, and to applications such as obsidian hydration dating.

It has been known for several decades that the chemical diffusion coefficient of "water" in silica glass and other compositionally simple silicate glasses increases strongly with the water content of the glass (e.g., DRURY and ROBERTS, 1963; COCKRAM et al., 1969; BURN and ROBERTS, 1970; LANFORD et al., 1979; HOUSER et al., 1980; TSONG et al., 1980; NOGAMI and TOMOZAWA, 1984). More recently, similar behavior has been documented for rhyolitic liquids with water contents up to 6 wt% (SHAW, 1974; JAMBON, 1979, 1983; DELANEY and KARSTEN, 1981; LAPHAM et al., 1984; STANTON et al., 1985). There has been much speculation on the cause of this strong concentration dependence of water diffusion in amorphous silicates. Some authors have suggested that it is related to the interdiffusion of cations and water molecules or hydronium ions (COCKRAM et al., 1969; DOREMUS, 1975; LANFORD et al., 1979; HOUSER et al., 1980; TSONG et al.,

1980); others have interpreted it as being due to the depolymerization of the silicate network upon dissolution of water as hydroxyl groups (HALLER, 1963; ROBERTS and ROBERTS, 1966; DELANEY and KARSTEN, 1981); still others have speculated that it is related to the fact that water dissolves in glasses and melts as two major species, H_2O molecules (hereafter H_2O refers to H_2O molecules; the word "water" is used to refer to total water) and hydroxyl groups (hereafter referred as OH) with different diffusion coefficients. Several authors have suggested that, although there are two hydrous species, only H_2O molecules are mobile in the melt or glass while OH and H_2O contents are related by interconversions between OH and H_2O (DOREMUS, 1969, 1973; ERNSBERGER, 1980; SMETS and LOMMEN, 1983; NOGAMI and TOMOZAWA, 1984; WASSERBURG, 1988; WAKABAYASHI and TOMOZAWA, 1989). OLBERT and DOREMUS (1983) suggested that during dehydration the diffusing species is molecular H_2O but that during hydration the diffusion is via alkali-hydronium interdiffusion. STANTON et al. (1985) ruled out the possibility of H_2 or H^+ being the diffusing species based on similarities in diffusion coefficients when hydration experiments by normal water and by deuterated water are compared. TOMOZAWA (1985) proposed that at low temperature OH is the diffusing species and at high temperature H_2O is the diffusing species. CHEKHMIR et al. (1988) assumed that OH is the dominant diffusing species below 0.4 wt% water (hereafter, % refers to weight percent unless otherwise specified) and that diffusion of H_2O becomes more important with increasing water content. We note that, although most of the recent treatments focus on the importance to diffusion of the presence of both OH and H_2O in the glasses or melts, few of them (SCHOLZE et al., 1975; OLBERT and DOREMUS, 1983; STANTON et al., 1985) actually determined contents of both species and only STANTON et al. (1985) determined species concentration *profiles* in hydrous silicate glasses.

In this paper, we present new data on the diffusion of water in natural rhyolitic glasses in order to understand the speciation and transport problem. Our data differ from most previous studies in that we have determined the concentrations of both H_2O molecules and OH groups along the experimental diffusion profiles by infrared spectroscopic measurement of samples quenched to room temperature. Such data are basic for evaluating the importance of the presence of different H-bearing species to water diffusion. We also present a general theoretical treatment of the problem of the diffusion and local equilibrium of H_2O molecules and OH groups (similar to those of WASSERBURG, 1988, and CHEKHMIR et al., 1988) and show how data on concentration gradients in these species can be used to extract quantitative constraints on their diffusion coefficients. The role of speciation in diffusion is interesting not only because of its importance in understanding water transport but also because other components may be present in silicate glasses and melts in several different forms. Thus, insights obtained from working on the water diffusion problem may provide a basis for understanding the diffusion of other components in amorphous and crystalline silicates and for relating them to their structures and properties (ZHANG et al., 1990b).

EXPERIMENTAL AND ANALYTICAL METHODS

Dehydration Experiments

The basic approach used in this work was to study the diffusive transport of water from an initially uniform, approximately semi-infinite source with a boundary condition of zero concentration at its planar interface. Experiments were conducted by holding polished wafers of natural rhyolitic glass (with a variety of initial water concentrations and speciation) in a N_2 gas stream at 1 atm total pressure at temperatures of 403–550°C for periods of 10–50 days. After quenching, the samples were sectioned perpendicular to the polished face, and infrared spectroscopy was used to measure the concentrations of hydrous species in the glass as a function of distance from the interface through which water diffused out of the sample over the course of the experiment.

The samples of glass used as starting materials came from the Mono Craters in central California and had initial water contents between 0.2 and 1.7% (see Table 1 and NEWMAN et al., 1986, 1988). Natural glasses were used because large synthetic glass chips with uniform and high water concentrations were not readily available. Fragments of these natural glasses were cut into chips and then ground and polished on parallel surfaces to a typical final thickness of 1 to 4 mm prior to the experiment (Table 1). The width and length of these polished wafers were usually greater than 10 mm, so they can be treated as infinite in these dimensions. Based on infrared analyses, the starting materials were homogeneous to within 5% of the total water present. The speciation of water (i.e., the concentrations of H_2O and OH) in these starting glass chips differed in some cases among chips with the same water concentration. We attribute this to difference in thermal history. These differences in initial speciation had little effect on experimental results because a quasi-equilibrium speciation was reached in a relatively short time during experiments. Most starting glasses contained bands of microphenocrysts (<20 μm), tentatively identified by optical microscopy as plagioclase, biotite, and magnetite, but MC3b glasses were almost free of microphenocrysts. Starting glasses usually contained bubbles, with the number

Table 1. Experimental runs for water diffusion

		Duration	Initial conc. (wt%)			Thickness	Final conc. at center (wt%)			
Glass #	T°C	days	H2O	OH	Total*	(mm)	H2O	OH	Total	Comments***
3b-D5dif	550	13.8	0.067	0.43	0.50 (7)	1.12	0.078	0.37	0.45 (2)	a
KS-big**	540	0.21	0.20	0.58	0.79 (2)	11	0.23	0.60	0.83 (4)	rk
KS-D2	530	11.4	0.24	0.60	0.83 (3)	2.97	0.24	0.60	0.84 (3)	
PD-D5	530	11.4	0.01	0.19	0.20 (1)	3.24	0.012	0.17	0.18 (3)	
PD-D2	490	11.0	0.01	0.18	0.18 (3)	1.76	0.037	0.21	0.25 (1)	a,d,h,sr
KS-D3	490	18.6	0.21	0.59	0.80 (3)	3.90	0.25	0.57	0.82 (1)	
PD-D4	490	18.6	0.01	0.19	0.20 (1)	3.16	0.013	0.18	0.19 (2)	
KS-D5A	450	51.7	0.21	0.58	0.78 (1)	4.30	0.29	0.53	0.82 (1)	
MC3b-D4N	403	39.9	0.70	0.99	1.68 (2)	2.67	0.96	0.84	1.80 (1)	rb
MC3b-D4	403	39.9	0.46	0.84	1.29 (2)	2.50	0.67	0.71	1.38 (2)	
KS-D4A	403	39.9	0.19	0.58	0.77 (3)	4.28	0.26	0.56	0.82 (2)	

* Number in parentheses indicates the number of analyses.

** For the big chip KS-big, some small pieces from corners of the big chip were measured before the experiment; one wafer was cut and 4 points measured after the experiment. Consequently the initial and the final measurements were made on pieces that are about 5 mm apart.

*** Comments: a: the slab was not thick enough and the center concentration was altered slightly by diffusive loss or gain; d: deformed during the run; h: hydration experiment; rb: center of the sample turned red-brown during the experiment; rk: experiment to study reaction kinetics; sr: surface reaction.

of vesicles per volume increasing with water concentration: PD glass samples (0.2% water) were free of bubbles; MC3b-D5dif and KS samples contained few bubbles; other MC3b samples (>1.2% water) contained up to ~0.4 vol%. The presence of a small quantity of small bubbles and microphenocrysts had no major effect on experimental results, as evidenced by similar diffusion coefficients obtained for samples with different percentages of bubbles and microphenocrysts.

Experiments were conducted in two horizontal furnaces equipped with automatic temperature controllers. Each furnace was lined with a silica glass tube through which dry N_2 gas flowed from a tank during the experiment, both to inhibit oxidation of the sample by the atmosphere and to ensure that, if surface equilibrium between the sample and the N_2 atmosphere was achieved, the concentration of water at the glass surface would be essentially zero. Two or more glass wafers were placed together in the "hot spot" adjacent to a Type K thermocouple; the control thermocouple for each furnace was outside of the silica tube near the furnace windings. Temperature gradients within the silica tube were <0.1°C/mm in the vicinity of the hot spot at ~500°C. When samples were placed in the hot spot, the reading on the thermocouple in the hot spot inside the silica tube initially decreased by up to 50°C, but a steady temperature was reached in less than 5 min, after which time the difference in reading between the thermocouple at the hot spot inside the glass tube and the thermocouple outside the glass tube was typically less than 2°C. Temperature fluctuations over the course of the experiment were within ±5°C at 500°C. All the thermocouples used were calibrated against a thermocouple that had been calibrated against the melting point of gold. The durations of the experiments were chosen to be long enough to produce a profile that could be conveniently measured by infrared spectroscopy (on the order of 500 to 1000 μm), but short enough so that diffusion can be approximated as having occurred within a semi-infinite medium, as roughly estimated from previous measurements of the bulk diffusion coefficient of water (KARSTEN et al., 1982). The glass wafers were quenched in ice + water.

Hydration Experiment

We also carried out an experiment in which rhyolitic glass was hydrated by exposing it to water vapor at elevated pressure and temperature. A doubly polished glass wafer with 0.2% initial water was placed with doubly distilled water in an annealed platinum capsule, which was then welded shut. The welded capsule was placed in a rapid-quench cold-seal pressure vessel and brought to 490°C and 250 bars. Excess water was present in the capsule throughout the experiment. Although the amount of water present as vapor in the capsule changed with time, P_{H_2O} inside the capsule is assumed to have been constant and the same as the pressure in the pressurizing medium (distilled water). After quenching, H_2O and OH concentrations were measured along the diffusion profile in the wafer, allowing us to determine water speciation. Although it was our intention to compare diffusion during hydration to that during dehydration, the initially doubly polished flat glass wafer deformed into a curved wafer with rough and white-powdered surfaces, so a good diffusion profile could not be obtained.

Experiments to Examine Water Reaction Kinetics

To determine the effect of quenching upon speciation, experiments were also conducted to examine the reaction kinetics of the interconversion of H_2O and OH in rhyolitic glasses. We used a range of natural glass wafers with different total water concentrations and wafers with similar total water concentration but different initial H_2O and OH concentrations. The wafers were held at elevated temperatures (400–600°C) for different times and then quenched and measured for H_2O and OH concentrations. We put fewer and smaller wafers in the furnaces in this set of experiments so that the temperature drop when they were put into the furnaces was small (<10°C) and a steady temperature was reached within 1 min or less than ¼ of run duration, whichever is shorter. Some results are presented here to examine whether species concentrations at experimental temperatures can be preserved after quench. The details of the experiments will be published elsewhere.

Infrared Analysis

After quenching, the wafer was sectioned perpendicular to its polished surface near its center (Fig. 1). This provided a glass slice with a complete diffusion profile. The slice was then polished on both sides and analyzed by infrared spectroscopy, in general following the procedures of NEWMAN et al. (1986). In the center of each slice (i.e., in a region of the sample least affected by water loss through the surface), a round aperture (600 μm in diameter) was used to delimit the infrared beam. However, over the region where diffusion was significant, a slit 10 μm wide and 2 mm long (Advanced Laser Systems, Inc., Waltham, Massachusetts, USA) was used. The slit was fixed to a translation stage and then a sample slice was mounted onto the stage. The stage was designed such that the slice could be rotated so that its rim was parallel to the slit, as well as moved in both vertical and horizontal directions by micrometer drives. The rim position of the wafer was determined by seeing it move into the slit with an optical microscope. Once the rim position was determined, the distance away from the rim was determined from the difference between the micrometer reading at the rim and the reading at the position measured; positions measured in this way are reproducible to better than 20 μm in a 1000 μm distance (the positions were independently confirmed by photographs taken after the measurements in a few cases; see Fig. 3). Note that although the slit width is only about 10 μm, the infrared beam diverges inside the sample and the effective width of the sample that is exposed to the beam may be considerably larger than 10 μm, depending on the sample wafer thickness. The convolution may affect the measured diffusion profiles (GANGULY et al., 1989). This effect on concentration profiles was examined by analyzing the same sample (PD-D5) thinned to different thicknesses (~600 vs. ~150 μm). No significant differences in the concentration profiles were found, but the data from the thinner wafers were much less precise due to smaller total absorbances and to interference fringes. Therefore, for most samples a thickness of 600 μm or greater was used to analyze the concentration profiles.

Water concentrations were determined from the infrared spectra obtained with a Nicolet 60SX FTIR. H_2O and OH concentrations were determined from the peak height of the absorption bands at 523.0 and 451.5 mm^{-1} using the molar absorptivities of NEWMAN et al. (1986). (All reported band positions vary by up to 1.0 mm^{-1} from sample to sample or from one point to another in the same sample.) Baselines were fit by smooth curves drawn with a french curve. Local glass densities were calculated iteratively considering the effect of water concentrations (SILVER et al., 1990). OH concentrations are reported as weight percent of H_2O that is present as OH. Total water contents were obtained by summation of the concentrations of these two species.

When total water concentration is low or the wafer is thin (for wafer thickness ≤ 150 μm), the absorption bands at 523.0 and 451.5 mm^{-1} may be too weak for their intensities to be determined precisely. In such cases, the peak height of the band at 357.0 mm^{-1}, which includes contributions from both H_2O and OH, was used to determine

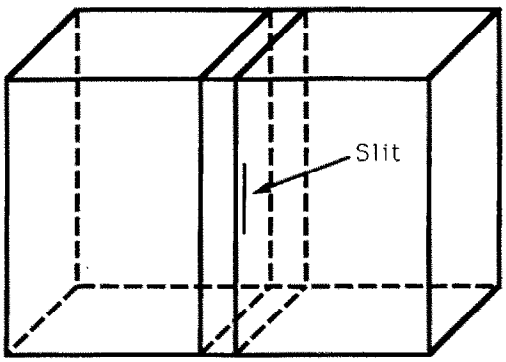

FIG. 1. Sketch of experimental charge (thickness between front and back surfaces is 1–4 mm; other dimensions are >10 mm, except for MC3b-D5dif which is about 6 mm in width and length).

total water concentration. We tried to avoid determining water concentrations using this band when the total water content is high (i.e., when both H_2O and OH contribute significantly to total water contents) because its molar absorptivity depends on both H_2O and OH contents (NEWMAN et al., 1986). However, at low water concentrations ($\leq$0.2%), total water concentration is assumed to be proportional to the peak height at 357.0 mm^{-1} with a molar absorptivity of 88 L/mol-cm (DOBSON et al., 1989) because H_2O concentration can be ignored (for the purpose of determining absorptivity) compared to that of OH at these low water levels. In a few cases a correction was applied for the growth in the detector of an ice band (325.0 mm^{-1}) in the course of the measurements.

Based on both the quality of the spectra and the reproducibility of an internal standard (sample POB1) that was analyzed many times along with the diffusion profiles, the relative precision of the analyses for total water and for OH is about 2–3% when a slit is used and about 1% when the 600 μm circular aperture is used. The relative precision for molecular H_2O depends on total water concentration because the fraction of water dissolved as H_2O depends strongly on total water concentration (while OH is usually the major species for the total water concentration range we have studied). The relative precision is about 3% at 1.5% water, 5% at 0.8% water, and 50% or worse at 0.3% water when the slit is used. When the 600 μm round aperture is used, the relative precision in molecular H_2O content is better than 2% at 0.8% water or more and about 20% at 0.2% water. Consequently, H_2O is difficult to measure near the sample edge (within $\sim$60 μm) due to low water concentration and because the precision cannot be improved by using a larger aperture. Another difficulty in measuring H_2O and OH concentrations near edges is that the edges of the polished slices are never perfectly flat due to chipping during cutting and polishing and/or due to surficial cracks (likely developed upon quenching and worsened during polishing). Therefore, H_2O and OH concentrations could usually only be measured at more than $\sim$30 μm away from the edge, the exact distance depending on the particular glass wafer.

Since water concentrations at the slice edge could not be directly measured due to these limitations, we confirmed that the water concentration at the edge for two charges (KS-D2 and KS-D3, both with initial $\sim$0.8% water) is essentially zero by the following method. The glass wafers were cut *parallel* to the face of the original polished wafer surfaces through which diffusion occurred and that slice was polished down to about 20 μm thick, where one side was the original exterior sample face. Average total water concentration in both slices was measured to be $\sim$0.1% based on the 357.0 mm^{-1} peak. (A number of points in KS-D3 were analyzed this way at different wafer thickness and results are shown as dotted squares in Fig. 3d.) Given that water concentration at 30 μm away from the edge is $\sim$0.3%, this value of $\sim$0.1% is consistent with an approximate surface water concentration of 0%. We therefore conclude that the water concentration at the edge is close to zero, approaching equilibrium with the dry N_2 ambient atmosphere.

Water concentration measured at the sample center after the experiment usually showed a slight (<5%) apparent *increase*, which we tentatively attribute to a small dependence of the molar absorptivities of H_2O and OH bands on thermal history. These small changes in molar absorptivities do not affect our interpretations of the diffusion profiles since these are based nearly entirely on relative concentrations, and small changes in speciation do not affect our results significantly. However, until these effects of thermal history are better understood, caution should be exercised in interpreting small variations (a few percent relative) of species concentrations in rhyolitic glass samples.

EXPERIMENTAL RESULTS

Water Concentration Profiles

A total of nine successful diffusive dehydration experiments were conducted at temperatures between 403 and 550°C on glasses with initial water contents between 0.2 and 1.7%. Experimental conditions are listed in Table 1. A series of representative spectra covering the concentration profile generated in sample KS-D3 measured with a 10 μm slit is shown in Fig. 2. Profiles in the concentrations of H_2O molecules, OH groups, and total water for all of the experiments are shown in Fig. 3. In all profiles, concentrations of both H_2O molecules and OH groups decrease towards the rim of the sample, but H_2O/OH ratios decreased with decreasing total water contents.

The smoothness of the profiles shown in Fig. 3 illustrates the precision of both the position and concentration measurements. Another test of the quality of our data is based on the fact that each slice prepared from experimental glass wafers has two edges through which water diffused during the experiment, and the diffusion profiles inward from both edges should be symmetric. Profiles inward from both edges were analyzed in two experimental charges (KS-D3 and PD-D5) and the data are superimposed in Fig. 3. In both cases, concentration profiles measured away from both edges are identical within a few percent, again illustrating the precision and internal consistency of both our concentration and position measurements.

We also measured major oxide concentrations across the water diffusion profile in KS-D2 (530°C, 11.4 d) using an electron microprobe. The concentrations of Na_2O and K_2O are plotted in Fig. 4 and show no systematic variations across the profile.

Potential Complications

Visible changes, including bubble formation and growth, deformation, and discoloration, occurred for samples with high initial water concentration over the course of some experiments. Data obtained on these samples were not used in our efforts to quantify water diffusion. New bubbles formed and/or old bubbles grew for samples with initial water concentrations > 0.7% at 550°C, >1.0% at 530°C, >1.2% at 490°C, and >2% at 403°C. These wafers also deformed to irregular shapes. Discoloration (possibly due to oxidation of ferrous iron to ferric iron by dissolved water) occurred for samples with initial water concentrations > 1.2% at 450°C, >1.5% at 403°C. If these effects proceeded too far, the experiments would be difficult to interpret, so we limit further

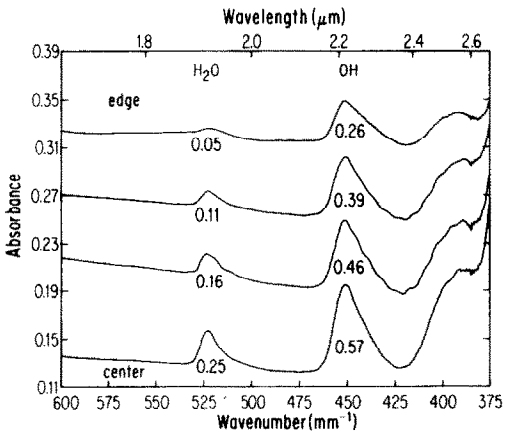

FIG. 2. A series of spectra from edge to center for KS-D3 (490°C, 18.6 d). H_2O and OH bands are at 523.0 and 451.5 mm^{-1}, respectively. Distances from the edge are 40, 120, 200, 530 μm. H_2O and OH concentrations (wt%) are given below the bands.

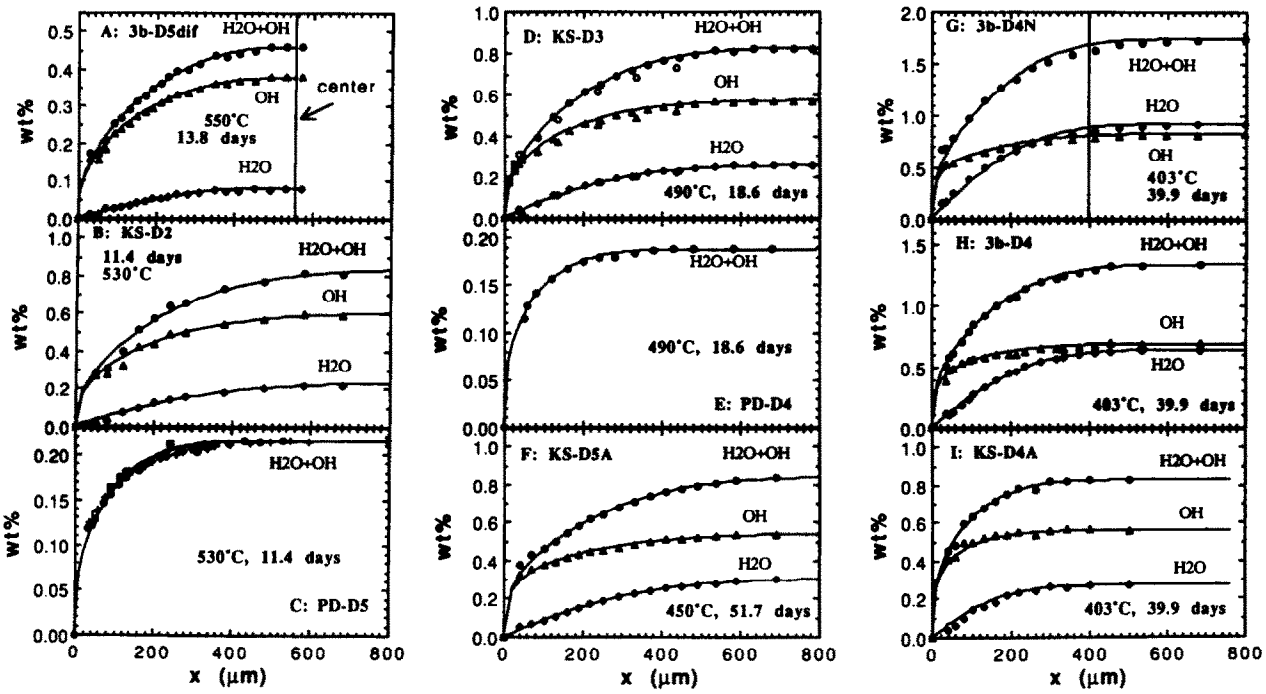

FIG. 3. Concentration profiles of H_2O, OH, and total water (H_2O + OH) for all experiments with best-fit curves based on our water diffusion model (D_{OH} = 0; see later discussion). Nicks on some of these curves (and in other diagrams) are due to the computer plotting program. For KS-D3 and PD-D5, profiles inward from both edges were measured and shown with filled symbols for concentrations measured from one edge and open symbols from the other edge. The curve fits for both KS-D3 and PD-D5 were for data represented by filled symbols only. For KS-D3, a number of points were also measured by polishing parallel to the diffusing surface, and those points were shown as dotted squares (near edge). For PD-D5, five points (shown as dotted squares) were measured for which the distances away from the edge were determined from photos taken after the measurements and an additional profile (shown as crosses) was measured on a wafer thinned to 140 μm. The vertical line in Fig. (g) (3b-D4N) marks the approximate transition between nearly colorless (near edge) and brown color (interior). For some samples there are measured points beyond the 800 μm limit used in this diagram which are not shown.

discussion of our experiments to the water concentration ranges reported in Table 1. For all samples reported in this paper, bubble sizes did not increase noticeably, and only one sample (3b-D4N, 1.7% initial water, 403°C) was slightly discolored after the experiment.

Our best data were obtained on the KS samples, which have initial water concentrations high enough (~0.8%) for us to measure both H_2O and OH precisely but low enough so that there are few bubbles before or after the experiments. Moreover, neither did these glasses deform nor were they discolored over the course of the experiments. For the PD samples, although they are clear, free of bubbles, and uncolored after the experiments, their H_2O concentrations could not be precisely determined before or after the experiments. Hence, data from them did not play a decisive role in the development of our water diffusion model.

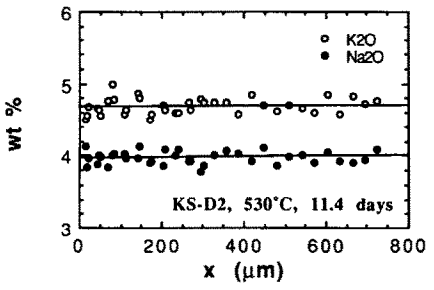

FIG. 4. Electron microprobe analyses of Na_2O and K_2O across the water diffusion profile for KS-D2 with 2 nA beam and 60 s counting time (1σ = 2% relative). Best-fit lines show that the slope is indistinguishable from zero.

The Effects of Quenching

Water speciation may be altered during quench of the experiments (STOLPER, 1989; SILVER and STOLPER, 1989; SILVER et al., 1990; DINGWELL and WEBB, 1989, 1991). Since both H_2O and OH concentrations are used in our modelling, knowledge of the extent of quench effects is essential for this study. It would be desirable to measure diffusion profiles at the experimental temperatures, but this is not routinely possible at present. Several experiments were run to study the kinetics of reactions by which OH groups are converted to H_2O molecules and vice versa. In one experiment, an 11 × 12 × 18 mm polished glass parallelepiped (compared to the 1 to 4 mm thick wafers for the diffusion experiments) with 0.8% total water concentration (KS-big in Table 1) was held at 540°C for 5 h and quenched in ice + water. The diffusion distance of water at 540°C in 5 h can be estimated to be ~50 μm based on our diffusion data. Based on thermal

conduction considerations (assuming a thermal diffusivity of 10^{-6} m^2/s), the center of the parallelepiped cools down to 300°C in ~30 s, while a point 300 μm away from the edge cools down to the same temperature in ~0.1 s. We measured a 4-point profile from the center to about 300 μm away from the edge and found no difference in speciation, demonstrating that for 0.8% water and 540°C the results are independent of average quenching rate between 10 and 2000°C/s. We assume the same result holds for samples with lower water contents and quenched from lower temperatures.

In other experiments designed to address this question, glass wafers with 0.5 to 2.6% dissolved water and with known initial species concentrations were held for various durations at elevated temperatures (400–600°C) and were then measured for H_2O and OH content after quenching. Figure 5 shows the variation of the parameter Q vs. time, where Q is defined as

$$Q \equiv \frac{[OH]^2}{[H_2O][O]}, \quad (1)$$

and O is anhydrous oxygens. Brackets in Eqn. (1) indicate mole fractions of OH and H_2O species expressed on a single oxygen basis and $[O] + [OH] + [H_2O] = 1$ (for calculation see STOLPER, 1989). At equilibrium, Q is equal to the equilibrium constant, K, for the following reaction:

$$H_2O + O \Leftrightarrow 2OH. \quad (2)$$

When possible, samples with initially different Q were chosen for this study so that equilibrium was approached from both directions (i.e., from below K and above K). At 500°C, parameter Q changed toward K by ~10% in 1 min for the two samples with 1.0 ± 0.1% water shown in Fig. 5a. At ~400°C, the only temperature at which we have samples with more than ~0.85% water, Q changed toward K by ~25% in 1 min for a sample with 2.6% water (Fig. 5b) and changed less than 2% in 5 min for a sample with 1.0% water. The highest initial water content for which we report diffusion experimental results is 1.7% at 403°C. Based on our kinetic data, we can infer that the change of Q toward K in 1 min at 403°C and 1.7% water would be less than 10%. At lower water contents the time to reach equilibrium is much longer (ZHANG et al., 1990a). Since the quench time scale is only several seconds based on thermal conduction considerations, we feel that the effect of quenching on the speciation in all our diffusion experiments can be at most a few percent and can be safely ignored.

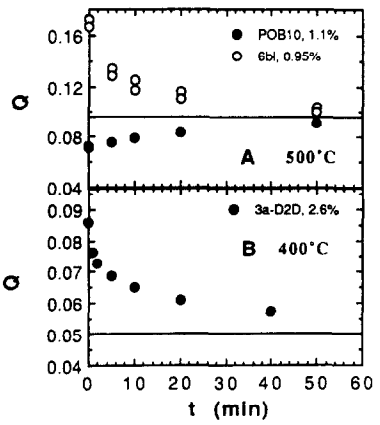

FIG. 5. $Q(\equiv[OH]^2/\{[H_2O][O]\})$ vs. time at (a) 500°C and (b) 400°C. Horizontal lines represent equilibrium K calculated from the equation given in caption of Fig. 6. Note that equilibrium is closely approached in about 1 h for the two samples at 500°C.

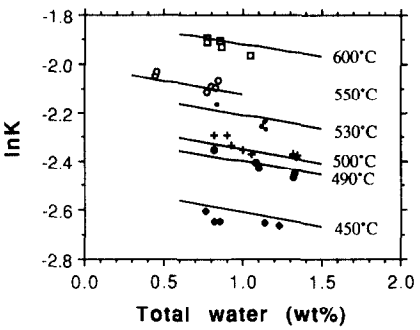

FIG. 6. ln K ($=[OH]^2/\{[H_2O][O]\}$ at equilibrium) vs. water concentration at the centers of experimental glass charges that are believed to have reached equilibrium at 550, 530, 490, and 450°C. Some equilibrium data based on reaction kinetics experiments at 600, 550, and 500°C are also shown. Relative errors on measured K are ~2% at >1% water and ~4% at 0.5% water. Calculated isotherms based on regular solution model fit of all equilibrium data are also shown. The equation for regular solution model (SILVER and STOLPER, 1989) based on our data set is given by

$$\ln K = A + (B + C[H2O] + D[OH])/T$$

where T is in K and $A = 1.409 \pm 0.166$ (2σ error); $B = -2816 \pm 118$; $C = -4448 \pm 2748$; and $D = -2721 \pm 3190$. $\Delta H_r^0 = -BR = 23.4 \pm 1.0$ kJ/mol where R is the gas constant.

Temperature Dependence of Equilibrium Speciation

The center of most samples was sufficiently far from the edges that it was unaffected by diffusion over the course of the experiment, but the speciation at the center was affected by reaction (2). All speciation data that are believed to have reached equilibrium based on a variety of criteria are presented in Fig. 6. The details of these equilibrium speciation data will be presented elsewhere. We note here that the speciation depends on temperature and that there is a slight dependence on total water concentration. Based on our studies of quenching effects (ZHANG et al., 1990a), we disagree with the assumption of DINGWELL and WEBB (1989, 1991) that all deviations from simple ideal behavior (i.e., from horizontal isotherms in Fig. 6) are due to speciation changes on quenching, which are enhanced at higher water contents. Our data are in general comparable to those of STOLPER (1989) at similar temperature and water content. These and other equilibrium data on reaction (2) have been fitted to a regular solution model (STOLPER, 1989; SILVER et al., 1990) with resulting parameters (see caption of Fig. 6) different from those of STOLPER (1989) and SILVER et al. (1990). Several calculated isotherms are shown in Fig. 6 and are used below to evaluate departures from local equilibrium along diffusion profiles.

Speciation along Diffusion Profiles and the Approach to Local Equilibrium

To examine whether local equilibrium is reached at each point along diffusion profiles (and at the centers of samples of low initial water concentration), we have compared the speciation along diffusion profiles and as calculated from the regular solution model mentioned in the preceding paragraph. In Fig. 7, we illustrate Q at the centers of experimental charges and along diffusion profiles at various temperatures and compare them with calculated equilibrium isotherm K (the expression for calculating these isotherms is given in the caption of Fig. 6). Note that Fig. 7b compares Q determined along diffusion profiles generated by both hydration and dehydration. Fig. 7 demonstrates clearly that at high water concentration and high temperature, Q in both hydration and dehydration experiments agrees with the equilibrium isotherms within error. However, at low water contents, Q is lower than K during hydration and higher than K during dehydration. Temperature is also an important factor in determining whether equilibrium is reached or not; i.e., for a given run duration, local equilibrium is only reached above a particular water concentration for a given temperature. Specifically, during dehydration, local equilibrium is approximately reached at water concentration $\geq$ 0.4% at 530°C (run duration 11.4 d), $\geq$0.5% at 490°C (18.6 d), $\geq$0.7% at 450°C (51.7 d), and $\geq$1.2% at 403°C (39.9 d). During hydration, local equilibrium is approximately reached at $\geq$1.3% water at 490°C (11.0 d).

DISCUSSION

Water Diffusion Models

In this section we discuss the calculation of diffusion coefficients (D_{H_2O} and D_{OH}) from the experimental data. We treat the diffusion of hydroxyl groups phenomenologically and are not concerned with how charges are balanced in the silicate structure. Given that OH groups and H_2O molecules may diffuse through a glass at different rates, characterized by D_{OH} and D_{H_2O}, respectively, it is possible to treat the water diffusion process by the following general equation (CHEKHMIR et al., 1988; WASSERBURG, 1988):

$$\frac{\partial[\text{water}]}{\partial t} = \frac{\partial}{\partial x}\left(D_{H_2O}\frac{\partial[H_2O]}{\partial x} + D_{OH}\frac{\partial[OH]/2}{\partial x}\right), \quad (3)$$

where [water], [H_2O], and [OH] are the mole fractions of total water, H_2O and OH, which, when calculated on a single oxygen basis, are approximately proportional to number densities (number of species per unit volume) of these species. The factor 2 in the above equation accounts for the fact that 2 moles of OH are equivalent to 1 mole of H_2O in terms of hydrogen; i.e., [water] = [H_2O] + [OH]/2. Given initial and boundary conditions, there are two methods to obtain the diffusion coefficients D_{OH} and D_{H_2O} from measured diffusion profiles and the above equation. The first is to solve Eqn. (3) numerically in a forward manner for [water], [H_2O], [OH] profiles as a function of $x/(D_{H_2O}t)^{1/2}$ given the ratio D_{OH}/D_{H_2O}. The solution can then be compared with measured concentration profiles to obtain D_{H_2O} from which D_{OH} can then be calculated. (If Eqn. 3 could be solved analytically, this method would be equivalent to fitting measured diffusion profiles by an analytical solution, such as an error function.) The second method is to use measured diffusion profiles to invert an integrated form of Eqn. (3) to obtain both D_{OH} and D_{H_2O} (the Boltzmann-Matano analysis). We use both approaches and we first discuss the forward solution method.

There are two independent unknowns in Eqn. (3), [H_2O] and [OH] (the third concentration variable, [water], is related to [H_2O] and [OH] by mass balance), which are to be solved as a function of x and t in a forward solution. Hence,

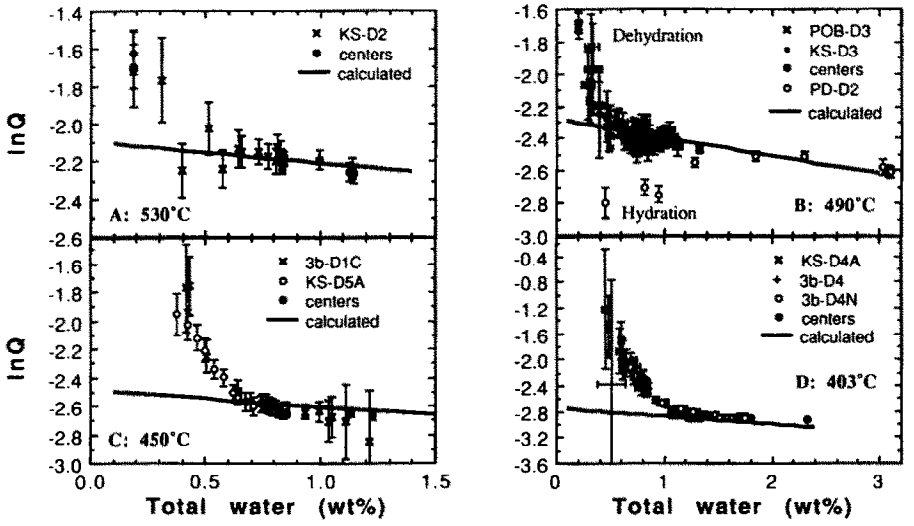

FIG. 7. Speciation (which may or may not be equilibrium speciation) at the centers and along the diffusion profiles for all samples at 530, 490 (including the hydration sample), 450, and 403°C, with reference lines from the regular solution model. Also shown are additional speciation data from samples in which new bubbles formed and/or old bubbles grew. Error bars represent calculated errors based on errors on H_2O and OH concentrations discussed in the text. Local equilibrium is reached at water concentration greater than 0.4% at 530°C for 11.4 d, 0.5% at 490°C for 18.6 d, 0.7% at 450°C for 51.7 d, and 1.2% at 403°C for 39.9 d.

one additional equation is necessary in order to solve for the concentration profiles given D_{OH} and D_{H_2O}. If there exists a relationship between [OH] and [H_2O], it can be combined with Eqn. (3) to solve the diffusion equation. The simplest calculation that we used was to use a constant Q obtained from the observed [OH] and [H_2O] in the interior of the sample (this is equivalent to assuming ideal solution and local equilibrium at all positions along the diffusion profile). The calculated curves were found to match the data quite well for initial water concentrations of more than ~0.8% at $D_{OH}/D_{H_2O} = 0$ (see footnote "d" of Table 3). This fit is much improved over what would be obtained by assuming a constant diffusion coefficient for total water. However, for samples with lower initial water concentrations (e.g., PD samples with 0.2%) there are small but substantial deviations. A modified model using K from a regular solution model that is weakly concentration dependent only improves the fit slightly. From Fig. 7 it can be clearly seen that at low total water content (i.e., near the edges of all samples and across the entire profile for samples with low initial water) the hydrous species are not in local equilibrium. Therefore, although these simple treatments are definitely in the right direction, they are not adequate at low water contents and temperatures.

To account for departures from local equilibrium along diffusion profiles, a general approach would combine Eqn. (3) with a knowledge of the temperature and concentration dependence of the kinetics of reaction (2), i.e., with a general equation for, e.g., $\partial[H_2O]/\partial t$, containing a diffusive flux term due to the local H_2O gradient and a reaction term due to local interconversion of OH and H_2O. Lacking a sufficiently detailed description of these kinetics, and noting that to a good first approximation all analyses of all dehydration samples at a given temperature fall on a single curve on Fig. 7, we have adopted an empirical description of the [OH] and [H_2O] relationship, formulated as Q (defined in Eqn. 1) as a function of [water] at a given temperature. The empirical expressions for Q are obtained from polynomial fits of the speciation data presented in Fig. 7 and are given in Table 2. As can be seen from Fig. 7, the empirical functions adopted are strong functions of water concentration at low water contents and approach the equilibrium distribution of species at water contents of 0.4 to 1.2%, depending on temperature (and run duration). We emphasize the limitations of the empirical functions we have adopted; for example, they are clearly not appropriate to the results of hydration experiments (Fig. 7b). Moreover, the speciation cannot in detail be a function of water content only but should also reflect initial speciation, the duration of the experiment, and the position in the diffusion profile. Nevertheless, as illustrated below, this approximation yields very good fits to our diffusion profiles and simple trends among the diffusion coefficients so determined.

Table 2. Empirical expressions for Q at various temperatures

$Q = a_{-1}/[\text{water}] + a_0 + a_1[\text{water}]$

where [water] is the mole fraction of total water and parameters a_{-1}, a_0, and a_1 at different temperatures are given below:

T(°C)	a_{-1}	a_0	a_1
550	0.000158	0.1056	0.3710
530	0.000287	0.1022	-0.5066
490	0.000489	0.0463	0.8012
450	0.001351	-0.0800	4.0264
403	0.001891	-0.0648	1.8264

In this expression for Q, Q is infinity at [water]=0 which does not produce difficulty in our calculation because [H_2O] and [OH] are both zero.

Diffusion Eqn. (3) and the empirical speciation relationships obtained above with a boundary condition of zero water concentration were solved numerically by making $D_{H_2O}t$ a new variable (τ) and given an assumed value of D_{OH}/D_{H_2O} (D_{H_2O} and D_{OH} were both assumed to be constant over the entire diffusion profile). We used an explicit forward finite-difference method (CRANK, 1975; PRESS et al., 1986) to solve Eqn. (3) with the associated expressions given in Table 2 to relate [H_2O] and [OH]. (Although implicit methods, such as the Crank-Nicholson method, are more stable and more accurate, they were not used because of the complex relationship between [water], [H_2O], and [OH] in Eqn. 3.) Using a time interval $\Delta\tau$ we calculated the profile at total diffusion time $j\Delta\tau$ where j is an integer. At each new time step $j + 1$, [water] as a function of x was calculated from [H_2O] and [OH] profiles at time step j using a finite difference form of Eqn. (3). Then [H_2O] and [OH] at time $j + 1$ were calculated using [water] at time $j + 1$ and the empirical speciation relationship. At each calculation a value of j and $2j$ were fixed for a given $\Delta\tau$. If there was a significant difference between the graph of [water] vs. $x^{(j)}/2\sqrt{j\Delta\tau}$ and [water] vs. $x^{(2j)}/2\sqrt{2j\Delta\tau}$, the calculation was repeated with $j_{new} \rightarrow 2j_{old}$ until the results converged for total times $j\Delta\tau$ and $2j\Delta\tau$. To insure stability, $(\Delta x)^2/\Delta\tau$ was chosen between 0.25 and 0.4 in the calculations. The numerical solutions were the same when different $(\Delta x)^2/\Delta\tau$ (0.25 to 0.4) were used and the solutions are smooth. The calculated diffusion profiles were then fitted to the actual diffusion profiles to obtain D_{H_2O} using a nonlinear minimization routine to minimize the following expression (i.e., to fit all three measured profiles by one single parameter D_{H_2O}):

$$S(D_{H_2O}) = \sum_i \left[\left(\frac{[\text{water}]_i - \widetilde{[\text{water}]_i}}{\sigma_{\text{water}}} \right)^2 + \left(\frac{[H_2O]_i - \widetilde{[H_2O]_i}}{\sigma_{H_2O}} \right)^2 + \left(\frac{[OH]_i - \widetilde{[OH]_i}}{\sigma_{OH}} \right)^2 \right], \quad (4)$$

where σ_j is error in $[j]$, and quantities with $\sim$ represent the values interpolated (using a second order polynomial) from diffusion profile tables from the forward calculation. D_{OH} is then calculated using the D_{OH}/D_{H_2O} ratio assumed in the forward calculation and D_{H_2O} obtained from the fit. In the fit, calculated concentrations far away from the edge are forced to be identical to the average of the measured concentrations near centers.

Best-fit Diffusion Coefficients

Figures 8a and b compare fits to the experimental diffusion profiles in sample KS-D3 (0.8% initial water, 490°C) for $D_{OH}/D_{H_2O} = 1$ and $D_{OH}/D_{H_2O} = 0$. Figure 8a ($D_{OH}/D_{H_2O} = 1$) corresponds to the case of simple total water diffusion so the calculated total water concentration vs. distance profile is proportional to a complementary error function. It is evident that the fit is a poor one in this case. Figure 8b shows that at $D_{OH}/D_{H_2O} = 0$ and constant D_{H_2O}, the fit to the data is excellent. To illustrate the dependence of the difference

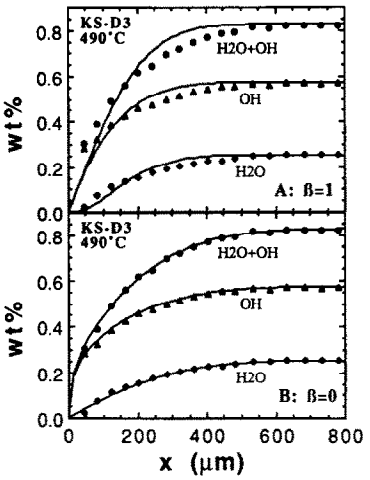

FIG. 8. Comparison of fits to water diffusion profiles of KS-D3 (490°C, 18.6 d) by the two species model for two extreme cases; β ($\equiv D_{OH}/D_{H_2O}$) = 1 and β = 0. H_2O + OH means total water. Q as a function of [water] is from Table 2. (a) D_{OH}/D_{H_2O} = 1, which is equivalent to a concentration-independent bulk water diffusion coefficient; (b) D_{OH}/D_{H_2O} = 0, for which molecular H_2O is the only diffusing hydrous species.

between the model calculated profiles and the observed profiles on the D_{OH}/D_{H_2O} ratio, we show fits for a range of D_{OH}/D_{H_2O} in Fig. 9a–c. Clearly the fit improves as the ratio decreases based on the figures. Figure 9d shows $1 - r^2$ (where r is the correlation coefficient; and $1 - r^2$ is proportional to S in Eqn. 4) of the fits for different values of D_{OH}/D_{H_2O}, which further illustrates the dependence of the quality of the fit on the D_{OH}/D_{H_2O} ratio for small D_{OH}/D_{H_2O} ratios. The minimum of the residuals lies near $D_{OH}/D_{H_2O} = 0$ ($D_{OH}/D_{H_2O} < 0.02$). The same procedure has been followed for PD-D5 (0.2% initial water, 530°C) and 3b-D4 (1.3% initial water, 403°C), and the minima of S of both were also found to lie near $D_{OH}/D_{H_2O} = 0$. The results for PD-D5 suggest that OH is not the dominant *diffusing species* even for samples in which OH is overwhelmingly the dominant *chemical species*. (If OH is both the dominant species and dominant diffusing species, the water profile should be proportional to a complementary error function if D_{OH} is constant, which is clearly not the case for our low water samples.) This result is contrary to the assumption of CHEKHMIR et al. (1988) that OH is the dominant diffusing species below 0.4% water content. For samples at lower temperature, the profiles themselves also clearly show that the OH diffusion coefficient is much smaller than that of H_2O (just judging from the length scale of the OH and of the H_2O profiles in Fig. 3).

We also employed a second, more direct approach to determining D_{OH} and D_{H_2O} from the measured H_2O and OH profiles in which we inverted Eqn. (3) using a Boltzmann transformation by replacing both x and t with a single parameter η ($\equiv x/2\sqrt{t}$; CRANK, 1975). With this transformation we obtain from Eqn. (3) the following:

$$-2\eta \frac{d[\text{water}]}{d\eta} = \frac{d}{d\eta}\left(D_{H_2O}\frac{d[H_2O]}{d\eta} + D_{OH}\frac{d[OH]/2}{d\eta}\right), \quad (5)$$

which upon integration from η_0 to ∞ becomes

$$D_{H_2O}\left(\frac{d[H_2O]}{d\eta}\right)_{\eta_0} + D_{OH}\left(\frac{d[OH]/2}{d\eta}\right)_{\eta_0} = 2\int_{[\text{water}]_{\eta_0}}^{[\text{water}]_\infty} \eta d[\text{water}]. \quad (6)$$

The integral on the right-hand side and the derivatives on the left-hand side can be evaluated numerically from the measured concentration profiles, although large errors may be associated with the numerical derivatives. Were it not for these large errors, Eqn. (6) could be used to solve for both D_{H_2O} and D_{OH} from two nearby points where the composition of the sample is essentially constant, and hence both diffusion coefficients can be regarded as constant. Notice that in order

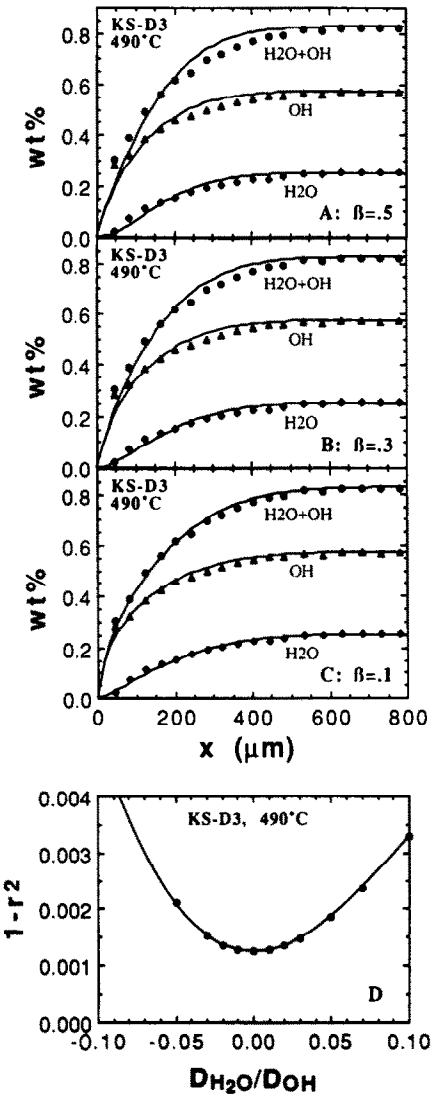

FIG. 9. Water diffusion profiles of KS-D3 fitted by the two species model for a range of β ($\equiv D_{OH}/D_{H_2O}$). H_2O + OH means total water. Q as a function of [water] is from Table 2. (a) D_{OH}/D_{H_2O} = 0.5; (b) D_{OH}/D_{H_2O} = 0.3; (c) D_{OH}/D_{H_2O} = 0.1; (d) $1 - r^2$ vs. D_{OH}/D_{H_2O}.

to solve for both D_{H_2O} and D_{OH} in this way, we would need large variations in the two derivatives that are not proportional. (Note that, from this argument, it is impossible to obtain diffusion coefficients of different species if their concentrations were proportional to each other, as they would be, for example, in CO_2-bearing glasses in which both CO_2 molecules and CO_3^{2-} are potential contributors to bulk carbon diffusion, but present in roughly constant proportions according to FINE and STOLPER (1985). The bulk diffusion coefficient for CO_2 in this case would be independent of the total CO_2 concentration, consistent with the results of WATSON et al. (1982). It is precisely the complicated nonlinear relationship between $[H_2O]$ and [OH] that allows us to determine D_{H_2O} and D_{OH}.) However, the two derivatives are always correlated (though not proportional) because of the local near equilibrium between H_2O and OH. In order to minimize the influence of these errors, we determined values of the two diffusion coefficients (assumed to be constant) to fit the entire profile using a simple linear least-squares procedure. D_{OH}/D_{H_2O} thus determined is very small (e.g., -0.05 ± 0.10 for KS-D3). This calculation confirms the conclusion presented above from fitting measured profiles with profiles calculated from Eqn. (3) using a forward difference method. However, the errors for both D_{H_2O} and D_{OH} are large with the direct approach compared to the fit of measured profiles to calculated profiles.

We conclude from the above analysis that our data are best explained by $D_{OH}/D_{H_2O} \approx 0$. It follows that the transport of water in rhyolitic glasses in the temperature and water concentration range we have studied is governed by the diffusion of H_2O molecules. The OH concentration profile is not due to the diffusion of OH groups, but due to the local interconversion between OH groups and H_2O molecules by reaction (2). The interconversion plays a critical role in supporting the local concentration of diffusing H_2O molecules. This result is consistent with the models of DOREMUS (1969), ERNSBERGER (1980), SMETS and LOMMEN (1983), NOGAMI and TOMOZAWA (1984), WASSERBURG (1988), and WAKABAYASHI and TOMOZAWA (1989). The result from analyzing diffusion profiles that $D_{OH} \ll D_{H_2O}$ is supported by comparing speciation during hydration and dehydration (Fig. 7b). During dehydration at low total water concentration the observed H_2O concentration at any point along a diffusion profile is lower than the equilibrium H_2O concentration, whereas during hydration it is higher. This suggests that during dehydration, H_2O is lost from a site (whereas during hydration it is added) and the conversion of OH to H_2O (or H_2O to OH during hydration) is necessary to bring the H_2O concentration to the equilibrium value. When the conversion is not rapid enough at low water concentrations, the H_2O concentration would be expected to be lower during dehydration and higher during hydration than the equilibrium value, as is observed.

Since D_{OH}/D_{H_2O} cannot be distinguished from zero, we adopt the approximation that $D_{OH}/D_{H_2O} = 0$ to treat all our data to obtain D_{H_2O} values. Table 3 lists the best-fit values for D_{H_2O} and the goodness of the fit for all our water diffusion experiments assuming $D_{OH} = 0$. The fits are compared with the measured profiles in Fig. 3. For the PD samples, only total water can be measured accurately from 357.0 mm^{-1} band; hence, only the [water] profile was fitted. For samples for which both H_2O and OH concentrations were measured, we obtain D_{H_2O} by fitting all three profiles (Eqn. 4), and we also report in Table 3 the range of D_{H_2O} values obtained by fitting [water] vs. x, or $[H_2O]$ vs. x, or [OH] vs. x individually. These ranges are usually within 10% of D_{H_2O} values obtained by fitting all three profiles. Errors on the best-fit D_{H_2O} values reported in Table 3 consider only misfit of the data and were obtained as described in CLIFFORD (1973; pp. 78–80) where the distance measurements are assumed to be error free. Real errors must be greater than those reported in Table 3 because there are other sources of experimental errors in determining D_{H_2O} that are difficult to evaluate quantitatively. For example, for some glasses with initial water greater than 0.85%, the presence of bubbles may affect the diffusion. At the other extreme, for glasses with initial water contents of 0.2% (PD-D4, PD-D5) and for all measurements near sample edges, the molecular H_2O concentration cannot be measured accurately and the empirical relationship between Q and [water] (Table 2) from which $[H_2O]$ is calculated is poorly constrained. More problematic is the fact that local equilibrium between OH and H_2O is not maintained along diffusion profiles for samples with low initial water concentrations and near sample edges. Although our empirical Q vs. [water] relationship corrects for this to some extent, it cannot do so entirely. We cannot evaluate the effects of these sources of errors on our fits, but the excellent fits of the profiles suggest that they are not major.

We infer that the dependence of D_{H_2O} on total water concentration is small because (1) the fits based on the assumption of constant D_{H_2O} account for whole profiles very well, and (2) best-fit D_{H_2O} values are similar for samples with different initial water contents. The total variation of D_{H_2O} is within ~40% at each temperature in our experimental concentration range. D_{H_2O} may be slightly higher for samples with higher initial water concentrations.

The dependence of D_{H_2O} on temperature is shown in Fig. 10. The activation energy for the diffusion of molecular H_2O is 109 ± 10 kJ/mol (2σ errors hereafter) based on a fit of all KS samples (~0.8% initial water) and is 92 ± 10 kJ/mol based on a fit of all our data to an Arrhenius relationship.

Table 3. Diffusion coefficients of molecular H_2O

Glass#	T (°C)	Initial water (wt%)	D_{H_2O}[a] (10^{-12} m^2/s)	D_{H_2O} range[b] (10^{-12} m^2/s)	$1-r^2$
3b-D5[c]	550	0.50	0.121 (0.005)	0.100-0.126	0.0022
KS-D2	530	0.83	0.115 (0.009)	0.113-0.117	0.0023
PD-D5	530	0.20	0.074 (0.008)	—	0.0060
KS-D3[d]	490	0.80	0.040 (0.001)	0.036-0.044	0.0012
PD-D4	490	0.20	0.045 (0.005)	—	0.0018
KS-D5A	450	0.78	0.0151 (0.0007)	0.0149-0.0152	0.0024
3b-D4N	403	1.68	0.0077 (0.0005)	0.0072-0.0077	0.0100
3b-D4	403	1.29	0.0073 (0.0002)	0.0068-0.0075	0.0011
KS-D4A	403	0.77	0.0050 (0.0005)	0.0035-0.0064	0.0041

All calculations assumed $D_{OH}=0$ and used speciation given by fits to Q given in Table 2. r is the correlation coefficient of the fit.

[a] 2σ errors for D_{H_2O} are in parentheses. These do not include errors associated with the fit to Q (given in Table 2) and associated with the assumption that $D_{OH}=0$.

[b] This column gives the range of D_{H_2O} obtained by fitting single concentration profiles: [water] vs. x, $[H_2O]$ vs. x, or [OH] vs. x.

[c] Water concentration at the center of this wafer was affected by diffusion and D_{H_2O} is calculated based on fit to a forward simulation of diffusion in *finite* space to account for the effect. Since the initial center water concentration relative to the final concentration is not known precisely (recall apparent water concentration at the center changes slightly during experiments due to dependence of absorptivities on thermal history, see text), there is an additional error associated with this fit which was not taken into account.

[d] $D_{H_2O}=0.036\pm0.002$ if constant $Q=0.095$ is used ($1-r^2=0.0032$); $D_{H_2O}=0.037\pm0.002$ if regular solution K is assumed ($1-r^2=0.0025$).

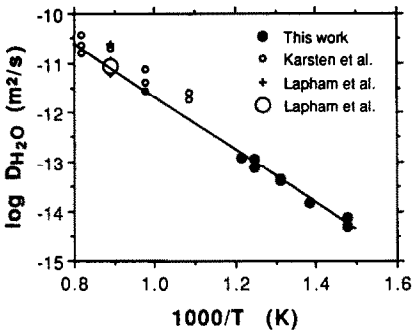

FIG. 10. Logarithm of the diffusion coefficient (m^2/s) of molecular H_2O vs. $1000/T(K)$. Uncertainties on D_{H_2O} of this study based on the fits (see Table 3) are smaller than the size of the points. Also plotted are previous data (small open circles for KARSTEN et al., 1982, and crosses for LAPHAM et al., 1984) where D_{H_2O} values were calculated from Eqn. (8) using K from caption of Fig. 6. The line is a best-fit drawn through all our data and a data point obtained by fitting the data of LAPHAM et al. (1984) using our model, shown as a large open circle. Activation energy for this line is 103 ± 5 (2σ error) kJ/mol.

Comparison to Previous Studies and Treatment of Previous Data

Most previous studies of water diffusion in rhyolites have been at higher temperatures than our experiments (i.e., on melts rather than glasses) and used hydration (SHAW, 1974; FRIEDMAN and LONG, 1976; ARZI, 1978; DELANEY and KARSTEN, 1981; KARSTEN et al., 1982; JAMBON, 1983; MICHELS et al., 1983; WHITE, 1983) or diffusion-couple (LAPHAM et al., 1984) experiments instead of dehydration experiments. Another difference with previous experiments is that previous authors determined either total water concentration profiles (DELANEY and KARSTEN, 1981; KARSTEN et al., 1982; JAMBON, 1983; LAPHAM et al., 1984) or total water losses during dehydration or gains during hydration (SHAW, 1974; JAMBON, 1979). When total water concentration profiles are determined, an apparent diffusion coefficient for total water (D^*_{water}) can be obtained from the following diffusion equation:

$$\frac{\partial[\text{water}]}{\partial t} = \frac{\partial}{\partial x}\left(D^*_{water}\frac{\partial[\text{water}]}{\partial x}\right). \quad (7)$$

This approach is equivalent to treating the diffusion of both species, H_2O and OH, with a single diffusion coefficient of D^*_{water} (which has to be a strong function of total water concentration to account for experimental data), and is clearly an oversimplification. When total water losses or gains are determined, a water diffusion coefficient that characterizes the mean transport rate over a range of water concentrations can be obtained. This diffusion coefficient is called $\overline{D^*_{water}}$ hereafter. $\overline{D^*_{water}}$ is not directly comparable to D^*_{water}. We now discuss how to treat other published data in the context of our two species diffusion model. We first compare our results with previous D^*_{water} data, and then treat previous $\overline{D^*_{water}}$ data.

Comparison with previous D^*_{water} data

In the context of our model (i.e., $D_{OH} = 0$), D^*_{water} and D_{H_2O} are related by (CHEKHMIR et al., 1988)

$$D^*_{water} = D_{H_2O}\frac{d[H_2O]}{d[\text{water}]}. \quad (8)$$

D^*_{water} at various water concentrations from diffusion profiles have been calculated in hydration (KARSTEN et al., 1982; JAMBON, 1983) or diffusion-couple (LAPHAM et al., 1984) experiments. Using Eqn. (8) we can calculate D_{H_2O} from the published values of D^*_{water}, given knowledge of the relationship between [H_2O] and [water]. Assuming local equilibrium at the high temperatures of these experiments, the species relationship was extrapolated from our equilibrium data at low temperatures and our estimate of the standard-state enthalpy change of reaction (2) (formula in caption of Fig. 6). From the D^*_{water} values of KARSTEN et al. (1982) and of LAPHAM et al. (1984), we have calculated D_{H_2O} at 650 to 950°C at water concentrations of 1 to 3%. These values of D_{H_2O} are shown in Fig. 10 and compared with our results obtained at lower temperatures. It can be seen that they are in reasonably good agreement. We have also calculated D_{H_2O} from D^*_{water} values of JAMBON (1983) at water contents of 1 to 6% after a hydration experiment at 750°C and 200 MPa water pressure. These D^*_{water} values are greater than those of KARSTEN et al. (1982, hydration at 70 MPa water pressure) at similar water contents, and the corresponding D_{H_2O} values (not shown) depend strongly on water content and are higher than the D_{H_2O} values shown in Fig. 10.

In addition, we have calculated a fit to the water concentration profile in the diffusion-couple experiments of LAPHAM et al. (1984) using our model of H_2O diffusion. We again assumed local equilibrium between H_2O and OH to relate the concentrations of the two species. The fit to the profile is shown in Fig. 11 and can be seen to be very good. (The interface in the fit is the Matano interface, instead of the actual interface. The Matano interface is the interface at which mass loss from one side equals the mass gain of the other side. The difference between the positions of the actual interface and the Matano interface is due to the Kirkendall effect; see SHEWMON, 1963.) The value of D_{H_2O} (9×10^{-12} m^2/s) at 850°C so determined lies almost exactly on the extension of our diffusion data (Fig. 10). If we combine this data point with all of our data, an activation energy of 103

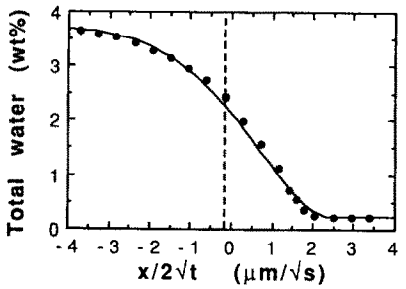

FIG. 11. Fit of the data of LAPHAM et al. (1984) at T = 850°C and P = 700 kbars (various durations) with our diffusion model assuming local equilibrium among species. The data were read from a smoothed curve from Fig. 2 of LAPHAM et al. (1984). K is extrapolated from Fig. 6. The interface in the fit is the Matano interface which is different from the actual interface (vertical dashed line) by 0.15 $\mu m/\sqrt{s}$ in $x/2\sqrt{t}$. The difference is due to the Kirkendall effect. D_{H_2O} obtained from this fit is shown as large open circle in Fig. 10.

$\pm$ 5 kJ/mol is obtained. The expression of D_{H_2O} at 400 to 850°C is

$$\ln D_{H_2O} = -(14.59 \pm 1.59) - (103000 \pm 5000)/RT \quad (9)$$

where D_{H_2O} is in m^2/s, T is temperature in K, R is the gas constant in $J\,K^{-1}\,mol^{-1}$, and errors are 2σ errors. As LAPHAM et al. (1984) carried out their experiments on hydrous silicate *melts* while ours were done on *glasses*, we take the excellent agreement to indicate that there are no detectable discontinuities or nonlinear changes in the $\ln D_{H_2O}$ vs. $1/T$ plot due to a glass-melt transition. This is consistent with the observations of JAMBON and SEMET (1978) that glass-melt transitions in silicate systems are difficult to detect in Arrhenius plots of diffusion data.

Based on our treatment, we can successfully reproduce the water diffusion profiles of LAPHAM et al. (1984) and can estimate the apparent total water diffusion coefficients D^*_{water} of KARSTEN et al. (1982) and LAPHAM et al. (1984). However, our model cannot reproduce the details of the water diffusion profiles from the hydration experiments of KARSTEN et al. (1982) and JAMBON (1983); neither can our model estimate D^*_{water} values of JAMBON (1983), which disagree with the results of KARSTEN et al. (1982). The profiles in both KARSTEN et al. (1982) and JAMBON (1983) deviate from an error function *more* than our model predicts, especially near the hydration surface. The failure of our model to predict the details of these water profiles cannot be totally due to the fact that these experiments were run at higher temperature in rhyolitic melts or due to errors in the local equilibrium assumption (which should be very good at these high temperatures anyway), given that we can reproduce well the water profiles produced in the diffusion-couple experiments of LAPHAM et al. (1984), which were conducted at similarly high temperatures. Neither can the failure be due to a contribution of OH to the diffusion of water in their experiments because this would make the total water diffusion profiles deviate *less* from an error function.

The discrepancy is possibly due to the very nature of hydration experiments, which differ somewhat from dehydration and diffusion-couple experiments. In dehydration and diffusion-couple experiments, the only major concentration gradients are in the H-bearing species. The gradients for other components are primarily due to dilution or enhancement by the addition or loss of water species. However, during "hydration," especially when the fluid phase is dense (at high pressures or in liquid water), both hydration (water dissolves and diffuses into silicate melt/glass) and leaching (silicates dissolve and diffuse out of the silicate into the fluid) occur due to partitioning of components between the two phases. Therefore, during hydration, both water and silicate components such as alkalies are mobile. Even though care was taken to minimize the dissolution and the leaching of the melt by placing rhyolite powders adjacent to the sample (KARSTEN et al., 1982), the effect might still be significant. Because the silicate components actively take part in the process, there may also be coupling between the diffusive components, in the form of interdiffusion (LANFORD et al., 1979) or multicomponent diffusion (which may show up as uphill diffusion, as observed by KARSTEN, 1982). Additionally, at low temperatures (<100°C), a gel-like reaction layer may form near the water-glass interface during hydration (DOREMUS, 1975). As we noted in the experimental section, in experiments in which we hydrated rhyolitic glasses at 490°C and 250 bars, we observed vapor-glass reaction at the interface (possibly due to dissolution and reprecipitation) and deformation of the interface. All these observations suggest that hydration experiments are more complicated and perhaps more difficult to interpret than dehydration or diffusion couple experiments. The above discussions are supported by the observations that no alkali concentration gradients were observed during dehydration (this study, Fig. 4) or during diffusion-couple experiments (LAPHAM et al., 1984), but that such gradients are generated during hydration experiments (WHITE, 1983; KARSTEN, 1982; and numerous studies on the hydration of commercial glasses; e.g., TSONG et al., 1980). We tentatively suggest that, because of diverse complex processes, the hydration results should not be directly compared to diffusion in dehydration or diffusion couple experiments, especially near the vapor-melt or liquid-glass interface. The effects of these complex processes may be more severe under higher water pressures, which may be the reason for the disagreement between the results of KARSTEN et al. (1982) and of JAMBON (1983). Nevertheless, from the agreement of the D_{H_2O} values calculated from KARSTEN et al. (1982; see Fig. 10), we conclude that the dominant diffusing water species during hydration of rhyolitic melt at high temperatures is probably the same as that during dehydration and diffusion-couple experiments (i.e., molecular H_2O).

Treatment of $\overline{D^*_{water}}$ values (mean water transport rate)

Many previous authors have studied total water loss during dehydration or gain during hydration and characterized their data in terms of a constant diffusion coefficient for total water, $\overline{D^*_{water}}$ (e.g., MOULSON and ROBERTS, 1961; SHAW, 1974; JAMBON, 1979). Such treatments are complicated by the fact that D^*_{water} is in fact not constant along a diffusion profile. In fact, for cases in which D^* varies with concentration, different values of $\overline{D^*}$ could result depending on which of several techniques are used to extract $\overline{D^*}$ from total mass gain or loss data (although each is valid for the case in which D^* is constant along the diffusion profile). These complications may be part of the explanation of why $\overline{D^*_{water}}$ during hydration of silica glasses is higher than that during dehydration under similar conditions (MOULSON and ROBERTS, 1961). We now show that such a discrepancy is to be expected from our treatment of water diffusion even for constant D_{H_2O} and K.

To obtain $\overline{D^*}$ from mass gain or loss data, the following equation, which applies to diffusion in a semi-infinite medium (CRANK, 1975, Eqn. 3.15, p. 32), is often used (e.g., JAMBON, 1979; MOULSON and ROBERTS, 1961):

$$\overline{D^*} = \frac{\pi}{4t}\left(\frac{M}{c_0 - c_i}\right)^2, \quad (10)$$

where c_0 and c_i are the surface and initial concentrations of the component, t is the duration of the experiment, and M is total mass loss or gain per unit area directly measured. M can also be calculated as follows given a concentration profile:

$$M = \int_0^\infty (c - c_i)dx. \quad (11)$$

Assuming D_{H_2O} is constant and defining $\xi \equiv x/2\sqrt{D_{H_2O}t}$, we can combine Eqns. (10) and (11) to give the following expression:

$$\overline{D^*_{water}}/D_{H_2O} = \pi\{M^*/([water]_0 - [water]_i)\}^2, \quad (12)$$

where M^* is calculated from the [water] profile from an integration similar to M in Eqn. (11) except that the integration is with respect to ξ. Using Eqn. (12), it is possible to relate $\overline{D^*_{water}}$ and D_{H_2O} during both hydration and dehydration.

We have calculated model water diffusion profiles for both hydration and dehydration assuming $D_{OH} = 0$ and constant K and D_{H_2O}. K was arbitrarily taken as 0.1. In order to be comparable to MOULSON and ROBERTS (1961) experiments, $[water]_0$ was taken to be 0.001 and $[water]_i$ to be 0 in the hydration calculation and vice versa in the dehydration calculation. Given K, $[water]_0$, and $[water]_i$, [water] as a function of ξ can be calculated and M^* can be found. We then find by applying Eqn. (12) to these two model profiles that $\overline{D^*_{water}}/D_{H_2O}$ for hydration is a factor of 1.73 times that for dehydration. This is similar to the factor of 2.5 in the values of $\overline{D^*_{water}}$ for hydration and dehydration reported by MOULSON and ROBERTS (1961). We note that this factor does not depend on D_{H_2O}, although it does depend on K, $[water]_0$, and $[water]_i$. The small difference between the model and measured factor could be due to our assumption that K is constant and the assumed value of K, local disequilibrium during hydration and dehydration (see Fig. 7b and our earlier discussions on disequilibrium), or experimental errors. That $\overline{D^*_{water}}$ is greater during hydration than during dehydration at the same D_{H_2O} and K can be explained as follows. The interface water concentration and hence D^*_{water} near the interface are high during hydration and low during dehydration, and the interface diffusive flux (which is proportional to D^*_{water} at the interface) controls the water mass gain or loss. Diffusion in the interior also plays a role, of course, and tends, following this line of reasoning, to lessen the difference in $\overline{D^*_{water}}$ during hydration and dehydration.

Temperature dependence of D_{H_2O}, D^*_{water} and $\overline{D^*_{water}}$

The temperature dependence (i.e., the activation energy) of D_{H_2O} will be approximated well by that of D^*_{water} determined at a fixed water content and by that of $\overline{D^*_{water}}$ determined under fixed surface and initial water contents even under circumstances in which the speciation of water is not well known. At low water concentrations, both D^*_{water} and $\overline{D^*_{water}}$ are inversely proportional to K, and D^*_{water} can be expressed as follows assuming constant K based on Eqn. (8) (see DOREMUS, 1969; WASSERBURG, 1988):

$$D^*_{water} = 8[water]D_{H_2O}/K$$

$$= 8[water](D_{0,H_2O}/K_0)e^{-(E-\Delta H^0_r)/RT} \quad (13)$$

where E is the activation energy of D_{H_2O} and ΔH^0_r is the standard state enthalpy change of reaction (2). Hence the "activation energy" of D^*_{water} at low water content is lower than that of D_{H_2O} by ΔH^0_r, which is ~23 kJ/mol (see caption of Fig. 6). The same applies for $\overline{D^*_{water}}$ at low water content. At higher water content, the activation energies of D^*_{water} and $\overline{D^*_{water}}$ are even more similar to that of D_{H_2O}. For example, at equilibrium, based on our regular solution model (Fig. 6), the effect of temperature-dependent K contributes to a spurious "activation energy" of D^*_{water} of only −12 kJ/mol and of $\overline{D^*_{water}}$ of only −13 kJ/mol at 1% total water and about −5 kJ/mol at 4% total water. Therefore, the activation energies of D^*_{water} and $\overline{D^*_{water}}$ will typically be 5 to 23 kJ/mol lower than that of D_{H_2O}, depending on water concentration.

When the activation energy of D^*_{water} is determined under a fixed P_{H_2O} (e.g., MOULSON and ROBERTS, 1961), it differs from that of D_{H_2O} not only by the temperature dependence in K, but also by the temperature dependence of water solubilities. Since K increases with temperature (Fig. 6) and total water solubilities at a fixed P_{H_2O} decrease with temperature (with ΔH^0_{water} of ~12 kJ/mol in silica glasses at P_{H_2O} ~ 0.09 MPa, MOULSON and ROBERTS, 1961; and ~ 5 kJ/mol in rhyolitic melts at P_{H_2O} ~ 70 MPa, KARSTEN et al., 1982; where ΔH^0_{water} is the standard state enthalpy change for total water dissolution into a silicate), both effects reduce the fraction of H_2O with increasing temperature and hence reduce the "activation energy" of $\overline{D^*_{water}}$. Depending on the value of ΔH^0_{water} for total water solubilities, the activation energy for $\overline{D^*_{water}}$ determined at constant P_{H_2O} could thus be significantly lower than that of D_{H_2O}. However, due to a low ΔH^0_{water} for total water solubilities in rhyolitic melts, the activation energy of $\overline{D^*_{water}}$ should also be only slightly lower than that of D_{H_2O}.

It is thus not surprising that the activation energies for water diffusion in rhyolitic glasses and melts determined from studies of the temperature dependence of D^*_{water} and $\overline{D^*_{water}}$ are generally similar to but usually lower than our value of 103 ± 5 kJ/mol (2σ errors); e.g., 54 ± 13 kJ/mol (SHAW, 1974), ~130 kJ/mol (ARZI, 1978), ~46 kJ/mol (JAMBON, 1979), and 80 ± 4 kJ/mol (KARSTEN et al., 1982) (these errors from previous authors are probably 1σ errors). If an adjustment of ~10 kJ/mol is added to the result of KARSTEN et al. (1982) to account for the difference between D^*_{water} and D_{H_2O}, it would bring their activation energy to ~90 kJ/mol, in better agreement with our result. In any case, the difference between our value and that of KARSTEN et al. (1982) is not much outside the experimental errors, giving an activation energy for molecular H_2O diffusion at 80 to 110 kJ/mol in the temperature range 400 to 950°C.

Diffusion of Hydroxyl

Our diffusion data and our analysis thereof strongly suggest that hydroxyl groups are essentially immobile compared to H_2O molecules under the conditions of our experiments (i.e., $D_{OH}/D_{H_2O} \ll 1$). Although other workers have reached different conclusions (TOMOZAWA, 1985; CHEKHMIR et al., 1988) and there may indeed be conditions under which OH diffusion makes an important contribution to water diffusion, a small diffusion coefficient for OH groups is, *a priori*, a reasonable result because OH groups are charged and may be strongly bound to silicate tetrahedra. If OH groups are bonded to Si or Al (WASSERBURG, 1957), the diffusive behavior of the oxygen in the SiOH or AlOH unit and hence of OH (assuming OH diffuses as a whole unit) may be most similar

to the self-diffusion of other non-bridging oxygens (however, see KOHN et al., 1989, for an alternative view of the local hydroxyl environments in albitic glasses). The self-diffusion coefficient of oxygen determined by ^{18}O and ^{16}O exchange experiments in dry diopside melt (in which non-bridging oxygen is dominant) is 6×10^{-11} m^2/s at 1650°C and 15 kbars (SHIMIZU and KUSHIRO, 1984). We can estimate the diffusion coefficient of non-bridging oxygens at 500°C in silicate glass to be on the order of 10^{-20} m^2/s by a gross extrapolation using this result and an activation energy of 250 kJ/mol (the activation energy of oxygen diffusion in jadeite melt; SHIMIZU and KUSHIRO, 1984). Given that our value for the diffusion coefficient of molecular H_2O or total water is on the order 10^{-14} m^2/s at 500°C, this would give $D_{OH}/D_{H_2O} \sim 10^{-6}$; it may thus not be surprising that the diffusion coefficient of OH is many orders of magnitude smaller than that of H_2O in rhyolitic glass at this temperature.

The relative contribution of H_2O and OH diffusion to apparent total water "diffusion" is not only related to the diffusion coefficients of H_2O and OH, but also to the relative proportions of H_2O and OH. Since the fraction of H_2O decreases rapidly with decreasing total water content, it can be seen from Eqn. (3) that the contribution of H_2O to total water "diffusion" becomes smaller when water concentration is lower. At some very low water concentration, it may be necessary to consider the contribution due to diffusion of OH even under the conditions of our experiments. In order to evaluate the relative contributions of H_2O and OH diffusion to total water "diffusion," we have derived the following by modifying Eqn. (13) to include D_{OH} (again assuming equilibrium and constant K and low water concentrations):

$$D^*_{water} \approx D_{OH} + 8D_{H_2O}[\text{water}]/K. \quad (14)$$

Hence, the contribution to D^*_{water} (i.e., the flux of total water) due to OH diffusion would be the same as that due to H_2O diffusion if [water] = $KD_{OH}/(8D_{H_2O})$. Assuming $K = 0.1$ (at ~500°C) and $D_{OH}/D_{H_2O} \sim 10^{-6}$, then the contribution of OH and H_2O diffusion would be identical at [water] $\sim 10^{-8}$. These arguments are in accord with our conclusion that even at total water concentration as low as 0.2%, or [water] ~ 0.0036 (where H_2O is minute compared to OH), the contribution of OH diffusion to total water "diffusion" is still negligible.

CHEKHMIR et al. (1988) assumed that at total water concentration lower than 0.4%, OH is the only diffusing species and obtained D_{OH} by equating it to D^*_{water} at these low water concentrations. They then calculated D_{H_2O} from D^*_{water} at higher water contents by subtracting the contribution from OH diffusion. Their calculations based on this assumption would indicate that $D_{OH} \geq D_{H_2O}$ at $T \leq 600$°C or at a viscosity $\geq 10^{10}$ poise (Fig. 3 in their paper), which is clearly inconsistent with our experimental results.

Comparison of H_2O Diffusion with Diffusion of Other Neutral Species

The diffusion coefficient of molecular H_2O can be compared to that of other neutral species, especially the noble gases. Noble gas diffusion coefficients in rhyolitic glasses have been determined previously for He at 192–267°C (JAMBON and SHELBY, 1980), Ne at 100–400°C in tektites (REYNOLDS, 1960), Ne at 200–700°C (MATSUDA et al., 1989), and Ar at 500–900°C (CARROLL and STOLPER, pers. comm.; MATSUDA et al., 1989). The activation energies for the diffusion of He (35 ± 7 kJ/mol), Ne (~59 kJ/mol based on REYNOLDS, 1960; 74 ± 9 kJ/mol based on regression of the data of MATSUDA et al., 1989, excepting two points that lie outside the trend), H_2O (103 ± 5 kJ/mol, based on this work and one data point from LAPHAM et al., 1984), and Ar (152 ± 10 kJ/mol, CARROLL and STOLPER, pers. comm.) are shown in Fig. 12 against their molecular radii. The activation energy E (kJ/mol) can be expressed as a function of the radii (r in Å) of these neutral molecular species:

$$E = 94(r - 0.31)^2, \quad (15)$$

in agreement with the elastic theory of diffusion (see JAMBON, 1982, for a review), although the parameters (94 kJ mol^{-1} Å^{-2} and 0.31 Å) are not the same as those of JAMBON (1982). The fact that D_{H_2O} follows the same relationship in an E vs. r plot as the noble gas elements suggests that molecular H_2O diffuses in a manner similar to the noble gases, which are generally thought to be relatively unbound species that reside in holes in the glass structure (SHACKELFORD and MASARYK, 1978; SHACKELFORD and BROWN, 1981).

CONCLUSIONS

Water dehydration experiments on rhyolitic glasses have been carried out under a N_2 atmosphere and various temperatures. Concentration profiles of both H_2O molecules and OH groups were measured by Fourier transform infrared spectroscopy. As found in previous studies, the measured water concentration profiles do not match expectations based on a single constant diffusion coefficient for total water. We have modelled the diffusion of water by the diffusion of two

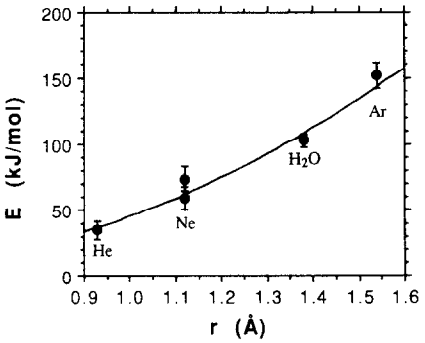

FIG. 12. Activation energies for the diffusion of molecular species He, Ne, H_2O, and Ar. Error bars represent 2σ errors. Data for He are from JAMBON and SHELBY (1980); for Ne are from REYNOLDS (1960) and MATSUDA et al. (1989); for H_2O are from this paper; and for Ar are from CARROLL and STOLPER (pers. comm.). The radius of H_2O molecules is estimated from distance of oxygen atoms in hexagonal ice structure to be 1.38Å (p. 465 in PAULING, 1960) which is not much different from the ionic radius of O^{2-} (1.40Å). The radii of the noble gases used (0.93 for He, 1.12 for Ne, and 1.54 for Ar) are the neutral atom radii (p. 643 in FORSYTHE, 1954). (If other sets of radii for noble gas atoms were used, a simple relationship between the activation energy of diffusion and the radii for H_2O and noble gas elements is not apparent.) The curve is a fit of the data to Eqn. (9) in JAMBON (1982) and is given by $E = 94(r - 0.31)^2$.

species: H_2O molecules and OH groups. It is assumed that the local abundance of these species is controlled by an interconversion by the reaction $H_2O + O \Leftrightarrow 2OH$, and an empirical relationship between speciation and total water concentration along the diffusion profiles was obtained from infrared measurements. The diffusion coefficients for both species were then calculated from the concentration profiles. Our results indicate that the diffusion coefficient of OH is negligible compared to that of H_2O at 400–530°C ($D_{OH} < 0.02 D_{H_2O}$ and could be much smaller), and OH does not contribute significantly to the diffusion of total water even at water concentrations as low as 0.2%, where the concentration of H_2O is minute compared to that of OH. The variation of OH concentration along the diffusion profile is inferred to be due to the local interconversion between OH groups and H_2O molecules. The reaction also provides the diffusing H_2O species. The conclusion that H_2O molecules are the predominant diffusing species at very low to high water concentrations confirms the results of several previous studies. D_{H_2O} values vary by less than a factor of two over the total water concentration range of 0.2 to 1.7%. The activation energy for diffusion of molecular H_2O is ~103 kJ/mol, and D_{H_2O} (in m^2/s) is given by

$$\ln D_{H_2O} = -(14.59 \pm 1.59) - (103000 \pm 5000)/RT$$

$$400°C \leq T \leq 850°C$$

where R is in J K^{-1} mol^{-1}. When compared with diffusion of noble gases, the diffusion coefficient of H_2O follows the same trend in an activation energy vs. radius plot. This supports the contention that what we call molecular H_2O behaves during diffusion as a *neutral molecular* species.

Acknowledgments—We thank Drs. W. L. Brown, D. B. Dingwell, and A. Jambon for insightful and constructive comments. YZ thanks Professor G. R. Rossman for his readiness to offer help in mastering the Nicolet 60X FTIR spectrometer, and Ms. Jackie Dixon and Dr. Sally Newman for their helping YZ to learn to use IR spectroscopy to measure water contents in silicate glasses. This is contribution 4851 (701) of the Division of Geological and Planetary Sciences, Caltech. This research is supported by NASA grant NAGW-1472 and NSF grant EAR-8916707 to EMS and DOE grant DE-FG03-88ER13851 to GJW.

Editorial handling: F. Albarède

REFERENCES

ARZI A. A. (1978) Fusion kinetics, water pressure, water diffusion and electrical conductivity in melting rock, interrelated. *J. Petrol.* **19**, 153–169.

BURN I. and ROBERTS J. P. (1970) Influence of hydroxyl content on the diffusion of water in silica glass. *Phys. Chem. Glass.* **11**, 106–114.

CHEKHMIR A. S., PERSIKOV E. S., EPEL'BAUM M. B., and BUKHTIYAROV P. G. (1985) Experimental investigation of the transport of hydrogen through model magmatic melts. *Geohkimiya* **5**, 594–598 (in Russian).

CHEKHMIR A. S., EPEL'BAUM M. B., and SIMAKIN A. G. (1988) Transport of water in magmatic melts. *Geohkimiya* **10**(2), 303–305 (in Russian).

CLIFFORD A. A. (1973) *Multivariate Error Analysis.* J. Wiley & Sons.

COCKRAM D. L., HAIDER Z., and ROBERTS G. J. (1969) The diffusion of water in soda-lime glass within and near the transformation range. *Phys. Chem. Glass.* **10**, 18–22.

CRANK J. (1975) *The Mathematics of Diffusion.* Clarenden Press, Oxford.

DELANEY J. R. and KARSTEN J. L. (1981) Ion microprobe studies of water in silicate melts: concentration-dependent diffusion in obsidian. *Earth Planet. Sci. Lett.* **52**, 191–202.

DINGWELL D. B. and WEBB S. L. (1989) The temperature-dependence of water speciation in rhyolitic melts: analysis of quench-rate dependent speciation using relaxation theory (abstr.). *Eos* **70**, 501–502.

DINGWELL D. B. and WEBB S. L. (1991) Relaxation in silicate melts. *Eur. J. Mineral.* (submitted).

DOBSON P. F., EPSTEIN S., and STOLPER E. M. (1989) Hydrogen isotopic fractionation between coexisting vapor and silicate glasses and melts at low pressure. *Geochim. Cosmochim. Acta* **53**, 2723–2730.

DOREMUS R. H. (1969) The diffusion of water in fused silica. In *Reactivity of Solids* (ed. J. W. MITCHELL); *Proc. 6th Intl. Symp.*, pp. 667–673. Wiley Interscience Press.

DOREMUS R. H. (1973) *Glass Science.* J. Wiley & Sons.

DOREMUS R. H. (1975) Interdiffusion of hydrogen and alkali ions in a glass surface. *J. Non-Cryst. Solids* **19**, 137–144.

DRURY T. and ROBERTS J. P. (1963) Diffusion in silica glass following reaction with tritiated water vapor. *Phys. Chem. Glass.* **4**, 79–90.

ELPHICK S. C. and GRAHAM C. M. (1988) The effect of hydrogen on oxygen diffusion in quartz: evidence for fast proton transients? *Nature* **335**, 243–245.

ERNSBERGER F. M. (1980) The role of molecular water in the diffusive transport of protons in glasses. *Phys. Chem. Glass.* **21**, 146–149.

FARVER J. R. and YUND R. A. (1989) The effect of H_2, O_2, and H_2O fugacities on oxygen diffusion in alkali feldspar (abstr.). *Eos* **70**, 501.

FINE G. and STOLPER E. M. (1985) The speciation of carbon dioxide in sodium aluminosilicate glasses. *Contrib. Mineral. Petrol.* **91**, 105–121.

FORSYTHE W. E., ed. (1954) *Smithsonian Physical Tables.* Smithsonian.

FRIEDMAN I. and LONG W. (1976) Hydration rate of obsidian. *Science* **191**, 347–352.

GANGULY J., BHATTACHARYA R. N., CHAKRABORTY S. (1989) Convolution effect in the determination of compositional profiles and diffusion coefficients by step scans. *Amer. Mineral.* **73**, 901–909.

HALLER W. (1963) Concentration-dependent diffusion coefficient of water in glass. *Phys. Chem. Glass.* **4**, 217–220.

HOUSER C. A., HERMAN J. S., TSONG I. S. T., WHITE W. B., and LANFORD W. A. (1980) Sodium-hydrogen interdiffusion in sodium silicate glasses. *J. Non-Cryst. Solids* **41**, 89–98.

JAMBON A. (1979) Diffusion of water in a granitic melt: an experimental study. *Carnegie Inst. Washington Yearbook* **78**, 352–355.

JAMBON A. (1982) Tracer diffusion in granitic melts: Experimental results for Na, K, Rb, Cs, Ca, Sr, Ba, Ce, Eu to 1300°C and a model of calculation. *J. Geophys. Res.* **87**, 10,797–10,810.

JAMBON A. (1983) Diffusion dans les silicates fondus: un bilan des connaissances actuelles. *Bull. Mineral.* **106**, 229–246 (in French).

JAMBON A. and SEMET M. P. (1978) Lithium diffusion in silicate glasses of albite orthoclase and obsidian composition. *Earth Planet. Sci. Lett.* **37**, 445–450.

JAMBON A. and SHELBY J. E. (1980) Helium diffusion and solubility in obsidians and basaltic glass in the range 200–300°C. *Earth Planet. Sci. Lett.* **51**, 206–214.

KARSTEN J. L. (1982) Potassium and sodium mobility during water diffusion in obsidian melts (abstr.). *Eos* **63**, 1137.

KARSTEN J. L., HOLLOWAY J. R., and DELANEY J. R. (1982) Ion microprobe studies of water in silicate melts: temperature-dependent water diffusion in obsidian. *Earth Planet. Sci. Lett.* **59**, 420–428.

KOHN S. C., DUPREE R., and SMITH M. E. (1989) A multinuclear magnetic resonance study of the structure of hydrous albite glasses. *Geochim. Cosmochim. Acta* **53**, 2925–2935.

LANFORD W. A., DAVIS K., LAMARCHE P., LAURSEN T., GROLEAU R., and DOREMUS R. H. (1979) Hydration of soda-lime glass. *J. Non-Cryst. Solids* **33**, 249–266.

LAPHAM K. E., HOLLOWAY J. R., and DELANEY J. R. (1984) Diffusion of H2O and D2O in obsidian at elevated temperatures and pressures. *J. Non-Cryst. Solids* **67**, 179–191.

LEE R. R., LEICH D. A., TOMBRELLO T. A., ERICSON J. E., and FRIEDMAN I. (1974) Obsidian hydration profile measurements using a nuclear reaction technique. *Nature* **250,** 44–47.

MATSUDA J. I., MATSUBARA K., YAJIMA H., and YAMAMOTO K. (1989) Anomalous Ne enrichment in obsidians and Darwin glass: Diffusion of noble gases in silica-rich glasses. *Geochim. Cosmochim. Acta* **53,** 3025–3033.

MICHELS J. W., TSONG I. S. T., and NELSON C. M. (1983) Obsidian dating and East Africa archeology. *Science* **219,** 361–366.

MOULSON A. L. and ROBERTS J. P. (1961) Water in silica glass. *Trans. Faraday Soc.* **57,** 1208–1216.

NEWMAN S., STOLPER E. M., and EPSTEIN S. (1986) Measurement of water in rhyolitic glasses: Calibration of an infrared spectroscopic technique. *Amer. Mineral.* **71,** 1527–1541.

NEWMAN S., EPSTEIN S., and STOLPER E. M. (1988) Water, carbon dioxide, and hydrogen isotopes in glasses from the ca. 1340 A.D. eruption of the Mono Craters, California: Constraints on degassing phenomena and initial volatile content. *J. Volcanol. Geotherm. Res.* **35,** 75–96.

NOGAMI M. and TOMOZAWA (1984) Diffusion of water in high silica glasses at low temperature. *Phys. Chem. Glass.* **25,** 82–85.

OLBERT B. H. and DOREMUS R. H. (1983) Infrared study of soda-lime glass during hydration and dehydration. *J. Amer. Ceram. Soc.* **66,** 163–166.

PAULING L. (1960) *The Nature of the Chemical Bond.* Cornell Univ. Press.

PRESS W. H., FLANNERY B. P., TEUKOLSKY S. A., and VETTERLING W. T. (1986) *Numerical Recipes.* Cambridge Univ. Press.

REYNOLDS J. H. (1960) Rare gases in tektites. *Geochim. Cosmochim. Acta* **20,** 101–114.

ROBERTS G. J. and ROBERTS J. P. (1966) An oxygen tracer investigation of the diffusion of "water" in silica glass. *Phys. Chem. Glass.* **7,** 82–89.

SCHOLZE H. (1988) Glass-water interactions. *J. Non-Cryst. Solids* **102,** 1–10.

SCHOLZE H., HELMREICH D., and BAKARDJIEV I. (1975) Behavior of soda-lime-silica glasses in dilute acids. *Glastech. Ber.* **48,** 237. (in German)

SHACKELFORD J. F. and BROWN B. D. (1981) The lognormal distribution in the random network structure. *J. Non-Cryst. Solids* **44,** 379–382.

SHACKELFORD J. F. and MASARYK J. S. (1978) The interstitial structure of vitreous silica. *J. Non-Cryst. Solids* **30,** 127–139.

SHAW H. R. (1974) Diffusion of H_2O in granitic liquids: Part I. Experimental data; Part II. Mass transfer in magma chambers. In *Geochemical Transport and Kinetics* (eds. A. W. HOFMANN et al.; *Carnegie Institute Washington Publ. 634,* pp. 139–170.

SHEWMON P. G. (1963) *Diffusion in Solids.* McGraw-Hill.

SHIMIZU N. and KUSHIRO I. (1984) Diffusivity of oxygen in jadeite and diopside melts at high pressures. *Geochim. Cosmochim. Acta* **48,** 1295–1303.

SILVER L. A. and STOLPER E. M. (1989) Water in albitic glasses. *J. Petrol.* **30,** 667–709.

SILVER L. A., IHINGER P. D., and STOLPER E. M. (1990) The influence of bulk composition on the speciation of water in silicate glasses. *Contrib. Mineral. Petrol.* **104,** 142–162.

SMETS B. M. and LOMMEN T. P. (1983) The role of molecular water in the leaching of glass. *Phys. Chem. Glass.* **24,** 35–36.

STANTON T. R., HOLLOWAY J. R., HERVIG R. L., and STOLPER E. M. (1985) Isotopic effect on water diffusivity in silicic melts: an ion microprobe and infrared analysis (abstr.). *Eos* **66,** 1131.

STOLPER E. M. (1982a) Water in silicate glasses: An infrared spectroscopic study. *Contrib. Mineral. Petrol.* **81,** 1–17.

STOLPER E. M. (1982b) Speciation of water in silicate melts. *Geochim. Cosmochim. Acta* **46,** 2609–2620.

STOLPER E. M. (1989) The dependence of the speciation of water in rhyolitic melts and glasses. *Amer. Mineral.* **74,** 1247–1257.

TOMOZAWA M. (1985) Concentration dependence of the diffusion coefficient of water in SiO_2 glass. *J. Amer. Ceram. Soc.* **68,** C251–C252.

TSONG I. S. T., HOUSER C. A., and TONG S. S. C. (1980) Depth profiles of interdiffusing species in hydrated glasses. *Phys. Chem. Glass.* **21,** 197–198.

WAKABAYASHI H. and TOMOZAWA M. (1989) Diffusion of water into silica glass at low temperature. *J. Amer. Ceram. Soc.* **72,** 1850–1855.

WASSERBURG G. J. (1957) The effects of H_2O in silicate systems. *J. Geol.* **65,** 15–23.

WASSERBURG G. J. (1988) Diffusion of water in silicate melts. *J. Geol.* **96,** 363–367.

WATSON E. B., SNEERINGER M. A., and ROSS A. (1982) Diffusion of dissolved carbonate in magmas: experimental results and applications. *Earth Planet. Sci. Lett.* **61,** 346–358.

WHITE A. F. (1983) Surface chemistry and dissolution kinetics of glassy rocks at 25°C. *Geochim. Cosmochim. Acta* **47,** 805–815.

ZHANG Y., STOLPER E. M., and IHINGER P. D. (1990a) Reaction kinetics of H2O + O = 2OH and its equilibrium revisited (abstr.). *Goldschmidt Conf.,* 94.

ZHANG Y., STOLPER E. M., and WASSERBURG G. J. (1990b) Role of water during hydrothermal oxygen diffusion in minerals (abstr.). *Eos* **71,** 650.